Hydrolytically-sensitive Hexaimino and Hydrolytically-inert Octaamino-cryptand Hosts for Dicopper†

Charles J. Harding,[a] Qin Lu,[a,b] John F. Malone,[b] Debbie J. Marrs,[a,b] Noreen Martin,[b] Vickie McKee[b] and Jane Nelson[a,b]

[a] *Chemistry Department, Open University, Milton Keynes MK7 6AA, UK*

[b] *School of Chemistry, Queens University, Belfast BT9 5AG, UK*

The hexa-Schiff-base cryptand $N[(CH_2)_2N{=}CH(C_6H_4\text{-}m)CH{=}N(CH_2)_2]_3N$ L^1 has been found to encapsulate a pair of Ag^I or Cu^I cations without hydrolytic attack on the imine bonds; a problem which is evident when the $[Cu^{II}_2(OH)]^{3+}$ assembly is incorporated. The structure of the dicopper complex of a singly ring-opened ligand, derived from L^1, has been determined. The octaamine cryptand L^2 (= L^1 + 12H) more easily accommodates a $[Cu_2(\mu\text{-}X)]^{3+}$ assembly where X = imidazolate, N_3^- or OH^-. Collinear disposition of the bridge with the N_{br}–N_{br} axis is confirmed in the first case by an X-ray crystallographic structure determination of the imidazolate-bridged cryptate, and inferred for the second case by spectroscopic and magnetic data, while, for the third case, magnetic susceptibility data indicate severe bending of the Cu–O(H)–Cu assembly.

Although square-based co-ordination is that commonly preferred by copper(II), other geometries, including trigonal-based co-ordination, are more frequently encountered in copper metalloprotein structures.[1,2] Our newly developed range of azacryptand hosts[3] represents a useful framework within which the chemical behaviour of copper in trigonal-based co-ordination sites can be studied and spectroscopically characterized.

The cryptand L^1, subject of the present study, functions as a dinucleating host with non-co-ordinating spacer links, allowing the co-ordination sites to be separated by around 4–5 Å. Repulsive interaction between the H_A protons means that L^1 is the most strained hexaimino macrobicycle of the azacryptand series, particularly in the convergent conformation adopted in its cryptate complexes.[4] Alone of the set of macrobicyclic ligands[3,5] generated by [2 + 3] condensation of the triamine tris(2-aminoethyl)amine, with 1,5- or 1,6-linked dicarbonyls, L^1 fails to template on metal cations, instead it crystallises out in the metal-free form. Once formed, however, the cryptand can be treated with Ag^+ or Cu^+ to give the binuclear cryptates $[Ag_2L^1][CF_3SO_3]_2\cdot 2EtOH$ **1** or $[Cu_2L^1]X_2\cdot nH_2O$ (X = ClO_4^-, n = 2 **2a**; X = BF_4^-, n = 3 **2b**) in high yield[6a] (Table 1). Indeed the copper(I) cryptate can be obtained by a pseudo-template method, provided that addition of Cu^+ is delayed until the triamine and dicarbonyl have reacted together for 15 min or so. The octaamine derivative, L^2 (= L^1 + 12H), with all six imino functions hydrogenated,[5,7] does not suffer from the same steric restrictions as L^1 and has previously been shown by Martell and co-workers[7] to accommodate a μ-1,3-CO_3^{2-} dicopper(II) assembly with a 5.85 Å separation of copper sites.

Results and Discussion

Hexaiminocryptates.—Proton NMR spectra of the disilver and dicopper complexes **1** *and* **2a**. The disilver (**1**) and dicopper (**2**) cryptates were obtained by treating the cryptand L^1 with the appropriate metal salt in ethanol–acetonitrile solution. Although crystals of **1** and **2** were too small for an X-ray crystallographic structure determination, ^1H NMR spectroscopy is able to furnish some structural information (Table 1). The expected conformational differences between the cryptates and free cryptand show up most clearly in the unique H_A aromatic signal, which is shifted dramatically downfield from the normal aromatic range in the cryptates, just as it is shifted upfield to the same extent in the free cryptand.[5] The resulting large (> 4 ppm) shift of H_A on complexation of L^1 reflects this proton's different experience of the cumulative ring current of three aromatic residues in the convergent, as against divergent, conformation. In the disilver complex **1** the H_A signal is considerably broadened at ambient temperatures, reflecting its involvement in some dynamic process. The methylene signals in **1** are likewise fluxional at ambient temperature, present as undifferentiated singlets with an intensity corresponding to four protons per cryptand strand, while at 233 K each methylene proton appears as either a poorly resolved, 2H (per strand) intensity triplet (if axial) or doublet (if equatorial). Another temperature-dependent feature of the ^1H NMR spectrum of **1** is the 8 Hz splitting of the H_D imino signal, seen only in the 233 K spectrum of **1** and absent in the dicopper analogue **2a**. Using other disilver cryptates of this series,[6,8,9] INEPT (insensitive nuclei enhanced by polarization transfer) experiments have demonstrated that such splitting of the imino resonance derives from three-bond coupling to $^{109,107}Ag$. The loss of this coupling at ambient temperature in **1** is the consequence either of cryptand mobility or of Ag^+ exchange between solvent and ligand, at a rate comparable with the NMR time-scale, *i.e.* appreciably faster than those for other 1,5-linked disilver cryptates of the series.[6,8,9] A lower $\Delta E^{\ddagger}$ for decomplexation, may reflect steric strain resulting from the accommodation of two relatively large Ag^+ cations in proximity to the three H_A aromatic protons. On the other hand, the smaller Cu^+ cation is expected to fit more easily into the cavity and the spectrum of $[Cu_2L^1][ClO_4]_2$ **2a** shows no sign of fluxionality (Table 1). The methylene resonances are well resolved at 294 and 233 K. The H_D imino signal remains unsplit at 233 K and the unique H_A aromatic proton appears as a sharp low-field singlet at both 294 and 233 K. The methylene-region of the spectrum of **2a** is more complex than those of the dicopper(I) cryptates of L^3 and L^5 which have already been reported;[9,10] however, the absence of splitting of the H_D resonance demonstrates that the complexity does not originate from an unsymmetric conformation in which the three strands or two ends of the macrobicycle are different.

† *Supplementary data available* (No. SUP 57078, 7 pp.): magnetic data. See Instructions for Authors, *J. Chem. Soc., Dalton Trans.*, 1995, Issue 1, pp. xxv–xxx.

Non-SI unit employed: G = 10^{-4} T.

Table 1 Proton NMR spectra of L^1, L^2 and derivatives[a]

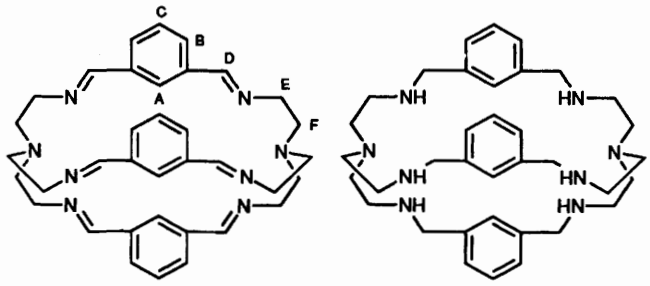

L^1 L^2

Compound	ν/MHz	T/K	Solvent	H_A	H_B	H_C	H_D	H_E		H_F	
1 $[Ag_2L^1][CF_3SO_3]_2 \cdot 2EtOH$	360	294	CD_3CN	9.48 (br s)	7.87 (d)[b]	7.75 (t)	8.59 (s)[c]	3.46 (t)[b,d,e]		2.90 (s)[e]	
		233	CD_3CN	9.58 (s)	7.84 (d)	7.76 (t)	8.63 (d)[f]	3.51 (t)	3.31 (d)	3.08 (d)	2.65 (t)
2a $[Cu_2L^1][ClO_4]_2$	400	294	CD_3CN	9.91 (s)	7.80 (d)	7.71 (t)	8.51 (s)	3.30 (d)	3.30 (d)	3.18 (d)	2.75 (m)
		233	CD_3CN	9.89 (s)	7.79 (d)[b]	7.70 (t)	8.50 (s)[c]	3.25 (m)[b]	3.25 (m)[b]	3.13 (d)	2.64 (m)
L^1	400	203	CD_2Cl_2	5.33 (s)	8.14 (d)	7.52 (t)	7.49 (s)	3.75 (q)	3.19 (t)	2.87 (t)	2.62 (q)
L^2	360	294	CD_2Cl_2	7.09 (s)	7.20 (m)	7.20 (m)	3.62 (s)	2.59 (m)[e]		2.45 (m)[e]	

[a] All shifts in ppm from $SiMe_4$. Integrals: H_A, H_C (1H); H_B, H_D, H_E, H_F (2H) per cryptand strand, unless otherwise indicated. [b] NOE enhanced. [c] NOE irradiated. [d] Poorly resolved. [e] Intensity (4H) per cryptand strand. [f] Coupling of 8 Hz.

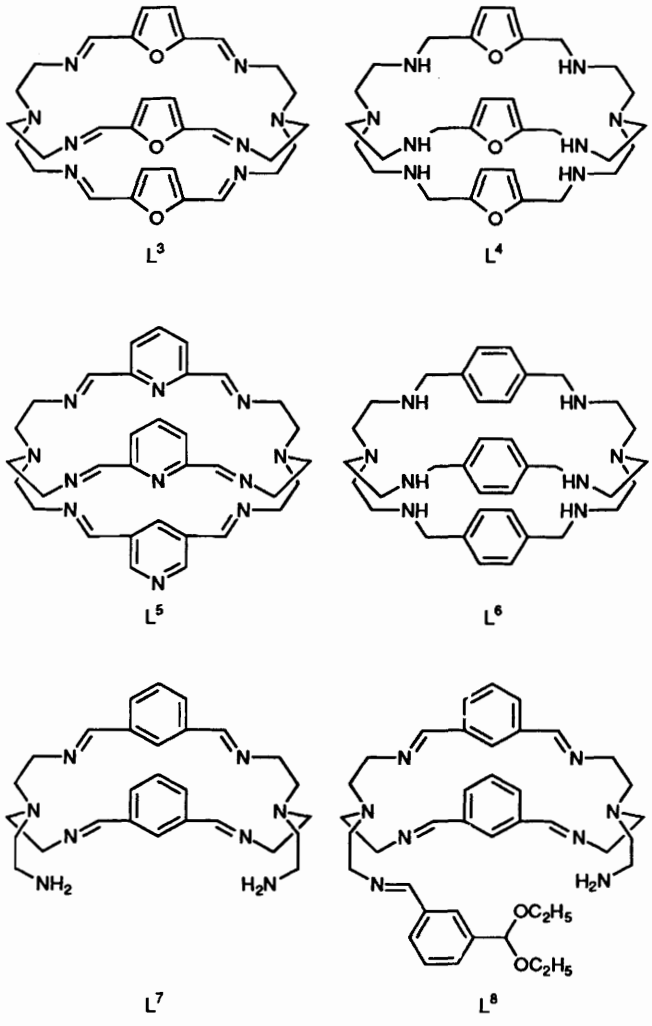

L^3 L^4

L^5 L^6

L^7 L^8

Instead, it seems that the accidental coincidence of some *vicinal* and *geminal* coupling constants which characterises other cryptates and free cryptands[3,5,8] has been lost. (This may be due to some alteration of torsion angles in the methylene caps.) Also, the overlap of $H_{E(ax)}$ and $H_{E(eq)}$ contributes to the complexity. At 298 K, these resonances appear as a broad doublet, but by 233 K have separated out somewhat into an irregular multiplet. An NOE (nuclear Overhauser effect) experiment involving irradiation into H_D enhances the high-field component of the H_E multiplet, which by analogy to other cryptate spectra[8-10] presumably corresponds to $H_{E(eq)}$.

Magnetic properties of the dicopper(II) complexes. The dicopper(I) L^1 cryptate requires no inert atmosphere protection in either dimethylformamide or MeCN, which is as expected given its relatively high redox potential[11] toward oxidation from the dicopper(I) state. Indeed, even treatment of **2** with Ag^+ as the oxidising agent fails to generate any copper(II). However, the free cryptand may be treated with hydrated copper(II) perchlorate to give a bright green microcrystalline solid, $[Cu_2L^1(OH)][ClO_4]_3 \cdot 2H_2O$ **3** (Table 2). Despite the obvious presence of the copper(II) chromophore (moderately intense d–d absorptions at 720 and 845 nm and an intense ligand-to-metal charge-transfer band close to 410 nm) no ESR spectrum is observable. Magnetic susceptibility measurements (Table 3, SUP 57078) confirm the virtual diamagnetism of this complex ($-2J \approx 800$ cm^{-1}), suggesting efficient antiferromagnetic exchange such as that existing[9,12] in $[Cu(OH)CuL]^{3+}$ ($L = L^3$ or L^4). In these cryptates X-ray crystallographic data confirm the existence of a linear [Cu–OH–Cu] assembly encapsulated within the cryptands. This means that the magnetic orbitals of copper(II), which are d_{z^2} in trigonal-co-ordination geometry, overlap well with the collinearly disposed O_{2p_z} orbitals of the bridge.

The only other bridged dicopper(II) complex of L^1 to be isolated, $[Cu_2L^1(N_3)][CF_3SO_3]_3$,[13] likewise has magnetic properties which indicate a collinear disposition of the magnetic orbitals and bridging link. In this case, however, the consequence of collinearity is orthogonality of the d_{z^2} magnetic orbitals with the highest occupied molecular orbital of the azide bridge, which rules out the possibility of antiferromagnetic exchange. Only weak ferromagnetic interaction is observed.

Hydrolysis of the Dicopper(II) Hexaiminocryptate **3**.—Despite repeated attempts, we did not succeed in incorporating bulkier bridging links such as imidazolate between the copper(II) cations in L^1. Indeed, even the bridged dicopper(II) complexes **3** and $[Cu_2L^1(N_3)][CF_3SO_3]_3$ which were obtained show signs

Table 2 Analytical, infrared and electronic spectral data for L^1 and L^2 and related complexes

Compound	Analysis[a] (%)			ν(C=N)/cm^{-1}		Electronic spectra[c]
	N	C	H	$\nu(NH_2)$/cm^{-1}	$\nu(X^-)$[b]/cm^{-1}	λ/nm (ε/dm^3 mol^{-1} cm^{-1})
1 $[Ag_2L^1][CF_3SO_3]_2\cdot 2EtOH$	9.3 (9.6)	40.9 (41.1)	3.9 (4.4)	1649m	1254, 1148, 1029s	—
2a $[Cu_2L^1][ClO_4]_2\cdot 2H_2O$	11.4 (11.8)	44.6 (45.6)	5.2 (4.9)	1646m	1086vs, 623ms	—
2b $[Cu_2L^1][BF_4]_2\cdot 3H_2O$	11.5 (11.9)	43.8 (43.9)	4.6 (5.1)	1626m	1081, 1060, 1025s	—
3 $[Cu_2L^1(OH)][ClO_4]_3\cdot 2H_2O$	10.4 (10.5)	40.7 (40.6)	4.0 (4.3)	1634m	1077, 1018vs, 622ms	355 (2800), 410 (4900), 720 (366), 845 (sh) (344)
4 $[Cu_2L^7(OH)][ClO_4]_3\cdot 2H_2O$	11.6 (11.6)	35.2 (34.8)	4.6 (4.6)	1646m	3314, 3273, 1093vs, 623ms	365 (4950), 610 (450)
5$\cdot 2H_2O$ $[Cu_2L^8(OH)][BPh_4]_2[CF_3SO_3]\cdot 2H_2O$	7.0 (7.1)	64.8 (65.9)	5.6 (5.7)	1643m	1247, 1167, 1028ms, 735, 707ms	400 (sh) (1500), 603 (450)
6 $[Cu_2L^2][ClO_4]_2\cdot 2H_2O$	12.0 (11.9)	46.1 (45.9)	5.7 (5.8)	3279m	1084, 1058vs, 621ms	—
7 $[Cu_2L^2(OH)][ClO_4]_3\cdot 3H_2O$	10.1 (10.2)	39.6 (39.5)	5.5 (5.6)	3255m	1122, 1108, 1089vs, 626ms	375 [1900 (sh)], 680 (325), 830 (420)
8 $[Cu_2L^2(N_3)][CF_3SO_3]_3$	12.3 (12.5)	37.9 (38.0)	4.3 (4.5)	3237m	2189ms,[d] 1250, 1160, 1026ms	404 (3000), 710 (427), 858 (517)
9 $[Cu_2L^2(im)][ClO_4]_3$	12.0 (12.3)	41.1 (40.9)	5.2 (5.5)	3251m	1093vs, 622vs	710 (469)

[a] Calculated values in parentheses. [b] X = CF_3SO_3, ClO_4, BF_4, OH or BPh_4. [c] In *ca.* 10^{-3} mol dm^{-3} MeCN, ligand-to-metal charge-transfer or d–d bands. [d] $\nu(N_3^-)$.

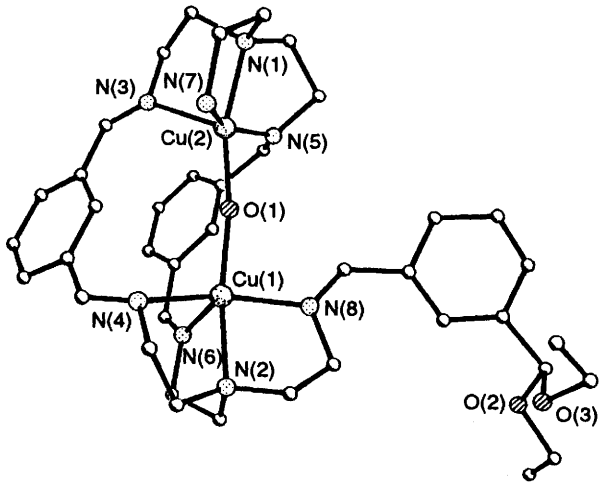

Fig. 1 Structure of the cation in complex **5**·H_2O·0.5EtOH

Table 3 Magnetic properties of the paramagnetic complexes (see also SUP 57078)

				μ^b/μ_B	
Complex	g	$-2J/cm^{-1}$	10^6 t.i.p.^{a}/cm^3 mol^{-1}	80 K	300 K
3	2.00	790	80	0.22	0.64
4	2.00	*ca.* 600^c	60	0.20	0.76
5	2.00	430^c	60	0.27	0.94
7	2.06	46	60	1.59	1.77
8	2.08	−25	60	1.92	1.84
9	2.05	111	80	1.11	1.65

^{a} t.i.p. = Temperature-independent paramagnetism. ^{b} Magnetic moment per Cu^{II} ion; $\mu_B \approx 9.27\,402 \times 10^{-24}$ J T^{-1}. ^{c} Poor fit to the Bleaney–Bowers' equation, these values of $-2J$ correspond to fixed values of $g = 2$ and t.i.p. = 60×10^{-6} cm^3 mol^{-1} in the fitting routine.

of strain in that they are not stable long term in solution: the initially bright green solution of $[Cu_2L^1(OH)]^{3+}$, for example, develops a blue colour on standing, owing to hydrolysis with a rate which is solvent- and counter ion-dependent. If complex **3** is left for 1–2 days in MeCN solution, particularly in the presence of CH_2Cl_2, a deep blue colour develops and crystals of dicopper complexes of the partially hydrolysed ligands L^7 or L^8 can be isolated. In the case of $[Cu_2L^7(OH)][ClO_4]_3$·$2H_2O$ **4**, this metal-assisted hydrolysis has resulted in the splitting off of an isophthalaldehyde molecule. The same blue product is obtained under inert atmosphere conditions, showing that this is a simple hydrolysis with no involvement of oxidative attack on the C–H_A bond.

The hydrolysis of complex **3** proceeds more slowly in the absence of CH_2Cl_2. Under these conditions, a dicopper(II) μ-hydroxo complex of the ring-opened ligand L^8, where just one imine function has been hydrolysed and solvent addition accompanying ring opening generates a terminal acetal function, can be crystallised out by addition of BPh_4^-. The blue-green complex $[Cu_2L^8(OH)][BPh_4]_2[CF_3SO_3]$·$H_2O$·0.5EtOH **5**·$H_2O$·0.5EtOH has been structurally characterised.

Structure and properties of $[Cu_2L^8(OH)][BPh_4]_2[CF_3SO_3]$·$H_2O$·0.5EtOH **5**·$H_2O$·0.5EtOH. Although the structural data for **5**·H_2O·0.5EtOH are of poor quality, they are sufficient to define the structure. The dipendant macrocycle L^8 has adopted a U-shaped configuration, containing the pair of copper(II) cations within the cleft. Both cations are in a distorted trigonal-bipyramidal co-ordination geometry (Fig. 1), using all available N-donors including one each (amino- or imino-N) from each of the pendant arms, with a bridging OH completing the co-ordination sphere. The Cu–O(H)–Cu angle

Table 4 Selected bond lengths (Å) and angles (°) for complex **5**·H_2O·0.5EtOH

Cu(1)–O(1)	1.943(9)	Cu(1)–N(8)	2.034(12)
Cu(1)–N(4)	2.073(11)	Cu(1)–N(2)	2.077(10)
Cu(1)–N(6)	2.279(10)	Cu(2)–O(1)	1.976(9)
Cu(2)–N(7)	2.009(13)	Cu(2)–N(5)	2.051(12)
Cu(2)–N(1)	2.126(12)	Cu(2)–N(3)	2.313(13)
O(1)–Cu(1)–N(8)	90.9(4)	O(1)–Cu(1)–N(4)	97.8(4)
N(8)–Cu(1)–N(4)	154.1(4)	O(1)–Cu(1)–N(2)	161.6(4)
N(8)–Cu(1)–N(2)	82.6(4)	N(4)–Cu(1)–N(2)	81.6(4)
O(1)–Cu(1)–N(6)	117.3(4)	N(8)–Cu(1)–N(6)	105.6(4)
N(4)–Cu(1)–N(6)	92.1(4)	N(2)–Cu(1)–N(6)	81.1(4)
O(1)–Cu(2)–N(7)	87.1(5)	O(1)–Cu(2)–N(5)	98.4(4)
N(7)–Cu(2)–N(5)	154.6(6)	O(1)–Cu(2)–N(1)	160.8(4)
N(7)–Cu(2)–N(1)	85.3(6)	N(5)–Cu(2)–N(1)	81.5(5)
O(1)–Cu(2)–N(3)	116.8(4)	N(7)–Cu(2)–N(3)	106.3(5)
N(5)–Cu(2)–N(3)	93.4(5)	N(1)–Cu(2)–N(3)	82.3(5)
Cu(1)–O(1)–Cu(2)	166.1(5)		

(Table 4) is 166.1(5)° and the Cu · · · Cu separation 3.89 Å. The pair of U-terminal aromatic rings are stacked, at an approximate separation of 3.4 Å, which presumably contributes to the stabilisation of this configuration. As in a related podand structure,[14] the acetal terminus of the pendant is directed away from the ligand cavity and makes no short intermolecular contact.

Table 4 shows that the distortion from trigonal-bipyramidal geometry is quite severe, with > 150° angles (which involve an imino- or amino-nitrogen donor from the pendant arms) evident in each equatorial plane. The N_{ax}–Cu–N_{ax} angle is nearly 20° off linear.

The near-linear Cu–OH–Cu assembly combined with the approximate trigonal-pyramidal co-ordination geometry evident in **5**·H_2O·0.5EtOH is associated with efficient antiferromagnetic exchange though appreciably less so than in complex **3**, where the Cu–O(H)–Cu angle necessarily lies nearer 180°. Although the temperature-dependence of the magnetic susceptibility of both complexes **4** and **5** makes a poor fit to the Bleaney–Bowers equation, it is clear that antiferromagnetic exchange in the dipendant amine macrocyclic complex **4** is very similar to that in **5** (Table 3).

The gradation of colour noticed in going from complex **3** to **5** to **4** suggests an alteration in the co-ordination geometry, and although the colour change is affected by the extent to which the intense $OH^- \longrightarrow Cu^{2+}$ charge-transfer transition lies in the visible part of the spectrum, there are also changes in the d–d absorption reflecting a change from trigonal-bipyramidal toward square-based geometry as the steric constraints of the cryptand framework are relaxed. For example, the pair of absorptions at *ca.* 700 and 850 nm, typical of trigonal-bipyramidal copper(II) geometry, is absent in **4** and **5**, being replaced by a single absorption close to 600 nm. However, distortion away from a regular trigonal-bipyramidal geometry does not appear to have had an important effect on the magnetic superexchange.

Octaamine (L^2) *Complexes of Copper*(I) *and Copper*(II).—The ready hydrolysis of dicopper(II) complexes of L^1 emphasises the unsuitability of this relatively strained hexaimine host for Lewis-acid guests such as copper(II), and draws attention to the possibility of replacing L^1 by the octaamine derivative L^2 where all six imino functions are hydrogenated.[5,7] This ligand is easily prepared by borohydride reduction of L^1, and readily co-ordinates copper in both oxidation states. Under inert atmosphere conditions, a colourless dicopper(I) complex, $[Cu_2L^2][ClO_4]_2$ **6**, is obtained, which rapidly acquires a green colour in solution or more slowly in the solid state on exposure to the atmosphere.

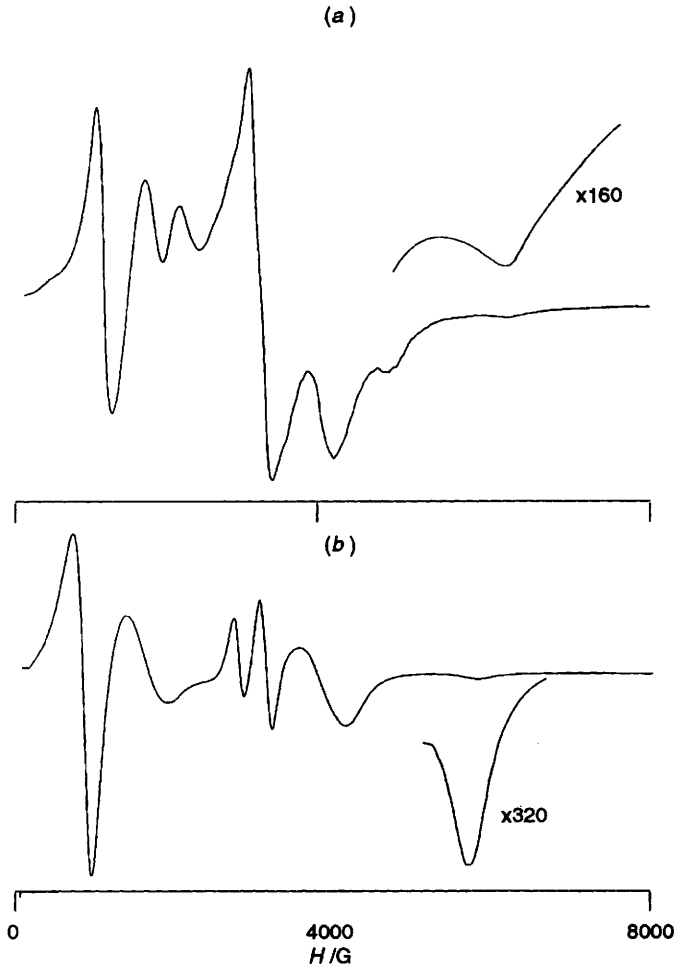

Fig. 2 The X-band ESR spectrum of $[Cu_2L(N_3)][CF_3SO_3]_3$ as a microcrystalline solid. (*a*) L = L^2, X-band 9.2428 GHz, 5 K; (*b*) L = L^1, X-band 9.2421 GHz, 7 K

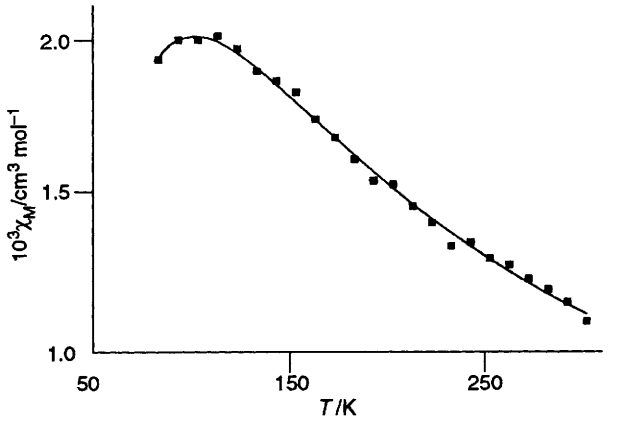

Fig. 3 The temperature dependence of the molar magnetic susceptibility (per Cu^{2+} ion) of **9** in the range 80 to 300 K; (■) experimental values, (——) Bleaney–Bowers' equation with $-2J$ = 111 cm^{-1}, g = 2.05

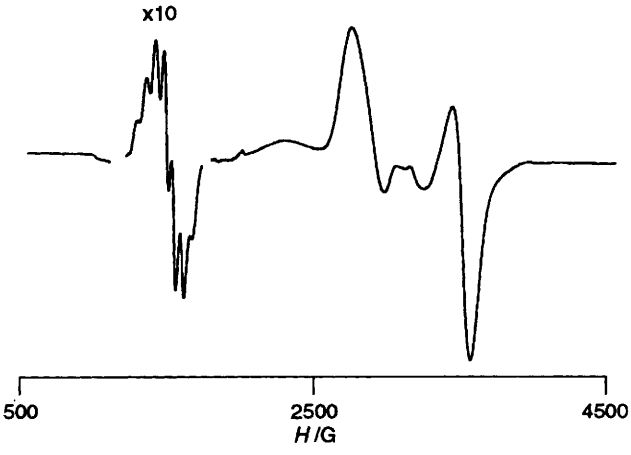

Fig. 4 The X-band (9.1586 GHz) ESR spectrum of complex **9** as a dimethylformamide glass at 100 K

Treatment of L^2 with copper(II) salts under mildly basic conditions generates pale blue crystals of the μ-hydroxo dicopper(II) complex $[Cu_2L^2(OH)][ClO_4]_3 \cdot 3H_2O$ **7**. An earlier report[7] infers, from the extremely low pK (4.58) of 2:1 stoichiometric mixtures of Cu^{2+}:L^2 in aqueous solution, the existence of a μ-OH^- linking the Cu^{2+} cations. The electronic spectrum of **7** shows a d–d absorption at *ca.* 830 nm with a shoulder at 680 nm (implying at least approximate trigonal-bipyramidal co-ordination geometry) together with a moderately intense ($\varepsilon \approx 1900$ dm^3 mol^{-1} cm^{-1}) 375 nm absorption appearing as a shoulder on the intense π–π* band. Signatures of strongly interacting μ-hydroxo-dicopper(II) in the azacryptand ligand series include[9,12] an intense absorption around 400–410 nm, together with a sharp infrared absorption above 3500 cm^{-1}, both of which are absent from the spectra of **7**. Magnetic susceptibility measurements on complex **7** confirm ($-2J$ *ca.* 46 cm^{-1}) the lack of strong antiferromagnetic interaction, suggesting that the $[Cu_2(OH)]^{3+}$ assembly held within L^2 is not linear. The dimethylformamide glass ESR spectrum confirms the presence of a weakish interaction in that the $g \approx 2$ signal is of normal intensity, but shows a poorly resolved $A_{\|}$ coupling of around 70–80 G in place of the usual 120–140 G; a weak half-band signal is also seen.

It is tempting to attribute the non-linearity of the Cu–O(H)–Cu assembly to steric hindrance of the three aromatic C–H_A bonds; in the more flexible L^2 host, an unsymmetric cryptand conformation which involves significant bending of the Cu–OH–Cu assembly, to avoid the close approach of the H_A protons, may be preferred. Hydrogen-bond interactions between the *sec*-amino nitrogen and hydroxo OH^- may also influence the Cu–O(H)–Cu angle, pulling the OH out of line to make a closer approach to one of the amino-nitrogen groups. On the other hand, it is possible that stabilizing π–π interactions[15] may apply whenever the guest anion incorporates a π system. On account of this and the greater flexibility of L^2, we expected that both triatomic bridging ligands, azide and imidazolate, could be incorporated between the co-ordinated copper(II) ions, and this expectation was fulfilled. In the azido-bridged complex $[Cu_2L^2(N_3)][CF_3SO_3]_3$ **8** we recognize the familiar spectroscopic characteristics[9,13] of azide linearly co-ordinated between copper(II) ions encapsulated within azacryptand ligands such as L^1, L^4 or L^6, *viz.*, a relatively high frequency infrared $\nu_{asym}(N_3^-)$ absorption (2189 cm^{-1}), a relatively low frequency $N_3^- \longrightarrow Cu^{II}$ charge-transfer absorption (404 nm) and a broad, extensively zero-field-split ESR spectrum with the most intense feature at unusually low field ($g \approx 6$) (Fig. 2). In addition, magnetic susceptibility measurements show the presence of a weak ferromagnetic interaction, with $-2J$ *ca.* -25 cm^{-1}.

The imidazolate-bridged complex, $[Cu_2L^2(im)][ClO_4]_3$ **9**, on the other hand, shows (Fig. 3) a moderately strong antiferromagnetic interaction ($-2J$ = 111 cm^{-1}) and a magnetic susceptibility *versus* temperature plot with the maximum close to 100 K. The ESR spectrum this time (Fig. 4) shows a normal triplet pattern with *ca.* 830 G zero-field splitting of the $D_{x,y}$ signals and a well resolved hyperfine-split (A_{iso} = 62 G) seven-line half band. The electronic spectrum (Table 2) shows a single unsplit maximum attributable to a d–d transition at 710 nm ($\varepsilon \approx 470$ dm^3 mol^{-1} cm^{-1}) suggesting a co-ordination geometry intermediate between square pyramidal and trigonal

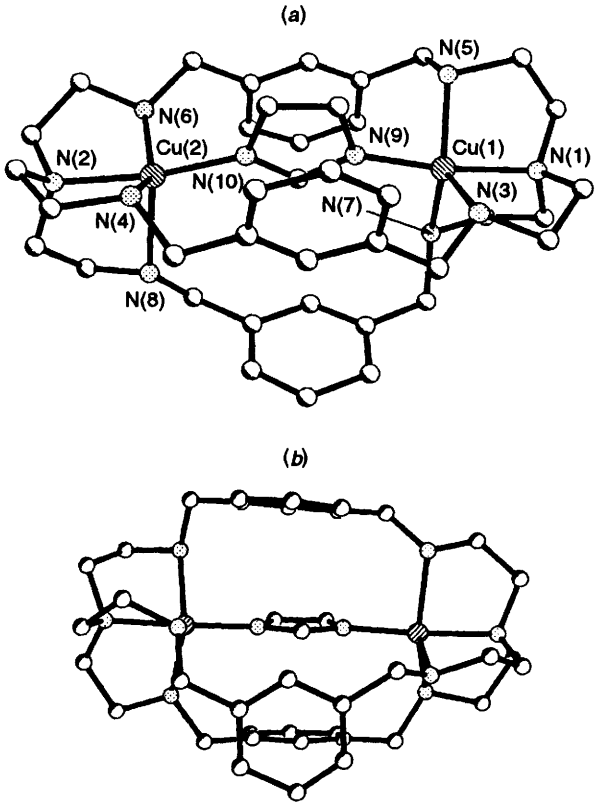

Fig. 5 (*a*) Structure of the cation in complex **9**; (*b*) a projection of complex **9** showing the aromatic ring stacking

bipyramidal. We were able to confirm this inference with an X-ray crystallographic structure determination of complex **9** (Fig. 5).

Structure of $[Cu_2L^2(im)][ClO_4]_3$ **9**. The bridged imidazolate ring is sandwiched between the aromatic rings of two of the cryptand strands. These three rings are almost parallel, but are offset by about 1.4 Å with respect to each other, *i.e.* they exhibit a parallel offset π–π attractive interaction as defined by Hunter and Sanders,[15] with an unusually short stacking distance of 3.05 Å. The aromatic ring of the third strand is almost perpendicular to the other three rings (79.2, 80.6, 86.4° respectively) and the conformation of the molecule places this ring in another energetically favourable relationship with one of the stacked aromatic rings: edge-to-face with an H • • • ring plane distance of 3.15 Å [Fig. 5(*b*)].

The distorted trigonal-bipyramidal co-ordination (Table 5) around each copper atom includes one Cu • • • N bond which is longer (*ca.* 2.3 Å) than the other four (*ca.* 2.0 Å), in each case the longer bond being to the nitrogen atom of the strand containing the non-stacked aromatic ring. At Cu(1) no interbond angle deviates by more than 15° from ideal trigonal-bipyramidal geometry, with N(1) and N(9) axial. The Cu(2) atom is somewhat closer to square-pyramidal geometry, with the apex on the longer bond [N(8)]. As expected from the relatively high value of the magnetic-exchange parameter in comparison with other μ-imidazolate complexes,[16] the Cu–N • • • N angles are not far from 180° [165 for Cu(1), 164° for Cu(2)]. There is no intramolecular or intermolecular hydrogen bonding.

This dicopper complex is isostructural with the corresponding copper–zinc complex reported recently.[17] This copper–zinc cryptate, prepared by adding one equivalent of Cu^{2+} to the monozinc L^2 cryptate, was refined by treating both cations as Cu^{2+}. The markedly different ESR parameters of complex **9** (Fig. 4), compared with the copper–zinc product ($A_{\|}$ = 1.45 × 10^{-2} cm^{-1}, $g_{\|}/A_{\|}$ = 152 cm), provide confirmation that the latter is not merely a dicopper complex deriving from 'scrambling' of Cu^{2+} and Zn^{2+} cations on mixing, but a genuine heterobinuclear complex.

Table 5 Selected bond lengths (Å) and angles (°) for complex **9**

Cu(1)–N(9)	1.93(2)	Cu(2)–N(10)	1.96(2)
Cu(1)–N(1)	2.02(2)	Cu(2)–N(2)	2.01(2)
Cu(1)–N(3)	2.10(2)	Cu(2)–N(4)	2.09(2)
Cu(1)–N(5)	2.111(14)	Cu(2)–N(6)	2.10(2)
Cu(1)–N(7)	2.251(14)	Cu(2)–N(8)	2.32(2)
N(9)–Cu(1)–N(1)	170.8(6)	N(10)–Cu(2)–N(2)	169.1(7)
N(9)–Cu(1)–N(3)	93.3(7)	N(10)–Cu(2)–N(4)	92.0(7)
N(1)–Cu(1)–N(3)	84.5(7)	N(2)–Cu(2)–N(4)	83.4(8)
N(9)–Cu(1)–N(5)	90.1(7)	N(10)–Cu(2)–N(6)	94.2(7)
N(1)–Cu(1)–N(5)	84.3(7)	N(2)–Cu(2)–N(6)	83.9(7)
N(3)–Cu(1)–N(5)	128.1(6)	N(4)–Cu(2)–N(6)	143.8(7)
N(9)–Cu(1)–N(7)	105.3(6)	N(10)–Cu(2)–N(8)	108.6(7)
N(1)–Cu(1)–N(7)	83.7(6)	N(2)–Cu(2)–N(8)	82.2(6)
N(3)–Cu(1)–N(7)	113.9(6)	N(4)–Cu(2)–N(8)	104.6(7)
N(5)–Cu(1)–N(7)	114.9(6)	N(6)–Cu(2)–N(8)	107.0(7)

Conclusion

As in the related L^3 and L^4 systems described earlier,[9,12] the hexaimine cryptand (L^1) is a good host for dicopper(I), but has more restricted dicopper(II) chemistry; we have succeeded in isolating only a strongly antiferromagnetically interacting μ-hydroxo- and a weakly ferromagnetically interacting μ-azido-dicopper(II) cryptate. The μ-hydroxo complex of the hexaimine cryptate is unstable long term in solution, generating derivatives of the ring-opened macrocyclic ligands, L^7 and L^8, following hydrolysis; the crystal structure of one of these has been determined.

The octaamine cryptand L^2 encapsulates Cu^I to give an air-sensitive dicopper(I) complex, but, in contrast to L^1, forms many stable dicopper(II) cryptates. The μ-azido-dicopper(II) cryptate of L^2, like its L^1 analogue, exhibits weak ferromagnetic interaction, and the μ-imidazolate cryptate which shows moderately strong antiferromagnetic interaction, has a structure involving stacking interactions between the imidazolate guest and the aromatic rings in the host. Compared with its L^1 analogue, the μ-hydroxo L^2 cryptate shows a markedly reduced antiferromagnetic interaction, which we attribute to the non-linearity of the Cu–O(H)–Cu assembly.

Experimental

Preparations.—L^1. Isophthalaldehyde (0.003 mol) was refluxed in MeOH (300 cm^3) until it dissolved when tris(2-aminoethyl)amine (tren) (0.002 mol) was added. After 30 min reflux, the solution was cooled and white crystals of L^1 were isolated in 90% yield.

$[Ag_2L^1][CF_3SO_3]_2$·2EtOH **1**. The cryptand L^1 (0.17 mmol) was dissolved in EtOH (50 cm^3) and an equal volume of MeCN added, followed by a solution of $Ag(CF_3SO_3)$ (0.3 mmol in 50 cm^3 1:1 MeCN–EtOH). The mixture was stirred at 40 °C for 6 h, filtered and the volume reduced to *ca.* 50 cm^3. On standing for several days in a freezer at −20 °C, a fine crystalline solid was obtained in 32% yield. FAB clusters at *m/z* 693 (base peak, AgL^1) and 951 [6.8%, $Ag_2L^1(CF_3SO_3)$] confirmed the encapsulation of silver cations.

$[Cu_2L^1]X_2$·nH_2O (X = ClO_4^-, n = 2 **2a**; X = BF_4^-, n = 3 **2b**). The cryptand L^1 (0.2 mmol) was dissolved in CH_2Cl_2 under inert atmosphere conditions and $[Cu(MeCN)_4]ClO_4$ (0.4 mmol) dissolved in deoxygenated MeCN–EtOH (2:1, 20 cm^3) added. Once the bright yellow colour showed that the complex had formed, the volume was reduced to 15 cm^3 under nitrogen and the complex isolated in 50% yield.

$[Cu_2L^1(OH)][ClO_4]_3$·$2H_2O$ **3**. The cryptand L^1 (0.5 mmol)

Table 6 Atomic coordinates (× 10^4) for complex **5**·H_2O·0.5EtOH

Atom	x	y	z	Atom	x	y	z
Cu(1)	1877(1)	366(1)	1819(1)	C(541)	−1631(9)	−3547(8)	−815(6)
Cu(2)	2878(1)	23(1)	3129(1)	C(551)	−1663(8)	−3408(8)	−332(6)
O(1)	2306(5)	300(5)	2503(4)	C(561)	−1024(7)	−3072(7)	−62(5)
N(1)	3205(7)	−50(8)	3909(5)	C(571)	218(7)	−2181(6)	551(5)
N(2)	1287(6)	760(6)	1182(4)	C(581)	−425(7)	−1730(6)	631(5)
C(1)	4022(9)	−291(10)	3934(7)	C(591)	−557(8)	−1423(8)	1130(5)
C(2)	4167(8)	−896(10)	3543(6)	C(601)	−43(7)	−1550(7)	1528(5)
N(3)	3991(7)	−628(7)	3027(5)	C(611)	577(8)	−1983(7)	1445(5)
C(3)	4375(9)	−877(10)	2664(7)	C(621)	681(8)	−2301(7)	958(5)
C(4)	4289(8)	−654(8)	2145(7)	C(631)	996(6)	−3215(6)	36(4)
C(5)	4675(9)	−1063(10)	1796(8)	C(641)	1762(7)	−3088(7)	95(5)
C(6)	4652(9)	−858(9)	1284(7)	C(651)	2265(8)	−3688(8)	202(5)
C(7)	4226(8)	−221(9)	1116(6)	C(661)	2023(9)	−4394(8)	261(6)
C(8)	3798(8)	170(7)	1471(6)	C(671)	1274(7)	−4569(8)	215(5)
C(9)	3831(7)	−47(8)	1978(6)	C(681)	784(7)	−3973(7)	90(5)
C(10)	3348(8)	806(8)	1297(6)	C(691)	718(7)	−1816(7)	−374(5)
N(4)	2726(6)	996(6)	1498(4)	C(701)	655(7)	−1041(6)	−253(5)
C(11)	2318(7)	1681(7)	1270(6)	C(711)	947(7)	−468(7)	−551(5)
C(12)	1722(8)	1362(8)	929(6)	C(721)	1312(7)	−629(7)	−980(5)
C(13)	2745(9)	−621(10)	4161(5)	C(731)	1396(8)	−1379(8)	−1111(6)
C(14)	2032(9)	−795(9)	3836(5)	C(741)	1125(7)	−1959(7)	−809(5)
N(5)	2298(6)	−947(7)	3311(5)	B(22)	3426(10)	1460(10)	5718(7)
C(15)	2335(7)	−1645(8)	3169(5)	C(752)	3257(9)	535(9)	5808(6)
C(16)	2626(8)	−1855(8)	2666(6)	C(762)	3698(11)	63(11)	6138(7)
C(17)	3081(8)	−2488(8)	2627(6)	C(772)	3549(12)	−725(12)	6201(8)
C(18)	3316(10)	−2714(9)	2163(7)	C(782)	2943(12)	−1052(13)	5944(8)
C(19)	3120(10)	−2308(9)	1727(6)	C(792)	2538(12)	−628(12)	5612(8)
C(20)	2659(7)	−1672(7)	1774(5)	C(802)	2679(11)	159(10)	5546(8)
C(21)	2415(8)	−1445(7)	2244(5)	C(812)	2581(8)	1852(8)	5623(6)
C(22)	2400(8)	−1272(9)	1301(5)	C(822)	2317(9)	2168(9)	5159(6)
N(6)	2072(5)	−640(6)	1290(4)	C(832)	1615(10)	2486(10)	5101(7)
C(23)	1806(7)	−374(7)	778(5)	C(842)	1139(10)	2507(9)	5496(6)
C(24)	1122(7)	125(7)	830(5)	C(852)	1347(9)	2185(8)	5945(7)
C(25)	3110(10)	743(11)	4097(8)	C(862)	2076(8)	1874(8)	6009(6)
C(26)	3409(12)	1344(11)	3736(8)	C(872)	3786(9)	1847(8)	6256(6)
N(7)	3149(9)	1133(7)	3192(5)	C(882)	3581(8)	1585(8)	6746(6)
C(27)	609(7)	1102(7)	1409(5)	C(892)	3867(8)	1973(8)	7189(6)
C(28)	244(7)	551(7)	1756(5)	C(902)	4338(10)	2581(9)	7154(7)
N(8)	829(6)	216(6)	2087(4)	C(912)	4564(9)	2843(9)	6700(6)
C(29)	653(9)	−59(9)	2500(6)	C(922)	4293(8)	2467(8)	6251(6)
C(30)	−120(10)	−110(10)	2755(6)	C(932)	3990(8)	1602(8)	5267(5)
C(31)	−77(11)	−197(12)	3282(8)	C(942)	4495(8)	1046(9)	5103(6)
C(32)	−770(14)	−190(14)	3553(9)	C(952)	4991(8)	1168(8)	4717(6)
C(33)	−1444(11)	−146(11)	3295(8)	C(962)	4997(9)	1846(9)	4483(6)
C(34)	−1469(10)	−110(10)	2790(7)	C(972)	4545(9)	2439(9)	4607(6)
C(35)	−807(9)	−119(9)	2528(7)	C(982)	4042(9)	2292(9)	5005(6)
C(36)	−2252(13)	56(9)	2564(8)	S(3)	1013(17)	2073(8)	2831(8)
O(2)	−2300(9)	−437(9)	2154(6)	O(113)	1705(14)	1848(14)	2582(9)
C(37)	−3110(14)	−379(14)	1851(10)	O(123)	228(24)	1713(32)	2706(19)
C(38)	−3123(18)	−1086(18)	1559(12)	O(133)	902(21)	2937(18)	2954(13)
C(36′)	−2252(13)	56(9)	2564(8)	C(1113)	1184(14)	1699(14)	3423(9)
O(3)	−2209(10)	772(10)	2293(7)	F(113)	1240(11)	928(11)	3417(8)
C(39)	−2359(17)	1500(16)	2632(12)	F(123)	1588(17)	2058(16)	3762(11)
C(40)	−1622(27)	1867(28)	2720(21)	F(133)	347(17)	1790(17)	3679(11)
B(11)	369(8)	−2512(8)	−37(5)	O(1)[S(3)]	454(19)	−496(19)	4816(13)
C(511)	−383(7)	−2866(7)	−305(5)	C(1)[S(3)]	217(19)	726(18)	5019(13)
C(521)	−411(9)	−3012(8)	−825(6)	C(2)[S(3)]	684(22)	318(23)	4820(15)
C(531)	−1019(9)	−3364(8)	−1086(6)	O(1)[W(3)]	4678(25)	1546(25)	2598(17)

was dissolved in CH_2Cl_2 and a solution of $Cu(ClO_4)_2$·$6H_2O$ (1.5 mmol) in the minimum quantity of EtOH was added, resulting in the precipitation of a bright green powder (80% yield). The filtrate starts to turn blue on standing for > 15 min. Rapid recrystallisation of the green powder from MeCN–EtOH gives a bright green microcrystalline product.

$[Cu_2L^7(OH)][ClO_4]_3$·$2H_2O$ **4**. The green powder **3** was redissolved in MeCN (100 cm^3) and left to stir overnight, gradually turning blue. (This colour change occurs more rapidly in the presence of CH_2Cl_2.) Slow evaporation of the blue reaction mixture gave thin blue lathe-like crystals of **4** in 30% yield. If this solution stands for more than a week at room temperature, a mixture of further hydrolysed products, including tren complexes, is obtained.

$[Cu_2L^8(OH)][BPh_4]_2[CF_3SO_3]$ **5**. To L^1 (0.2 mmol) in EtOH (80 cm^3) was added $Cu(CF_3SO_3)_2$ (0.4 mmol) in MeCN (20 cm^3), and the volume reduced to *ca.* 50 cm^3 before cooling in ice. Then $NaBPh_4$ (0.5 mmol) in EtOH (10 cm^3) was added, and the solution evaporated to yield blue-green crystals of **5**·$2H_2O$ in 30% yield. The recrystallised sample used for the X-ray crystallography had a slightly different solvation, **5**·H_2O·0.5EtOH.

L^2. A suspension of L^1 (3 mmol) was refluxed in EtOH (400 cm^3) and $NaBH_4$ added as solid in small amounts until no

Table 7 Atomic coordinates ($\times 10^{-4}$) for complex **9**

Atom	*x*	*y*	*z*	Atom	*x*	*y*	*z*
Cu(1)	6057(2)	2597(1)	5807(1)	C(7)	2458(20)	3964(11)	3966(14)
Cu(2)	2021(2)	1885(1)	4955(2)	C(8)	2546(22)	3726(11)	4685(16)
Cl(1)	2236(4)	−530(3)	6473(4)	C(9)	3434(21)	3747(10)	5283(14)
Cl(2)	6433(8)	4221(5)	3787(4)	C(10)	1753(18)	3434(14)	4840(16)
Cl(3)	678(6)	1864(6)	2148(5)	C(11)	322(21)	2705(14)	4238(16)
O(1A)	2028(17)	−1194(7)	6471(14)	C(12)	43(17)	2023(14)	4114(17)
O(1B)	1736(17)	−182(12)	6840(14)	C(13)	7918(16)	2309(12)	5811(13)
O(1C)	1974(15)	−312(11)	5697(9)	C(14)	7246(17)	2169(12)	4982(14)
O(1D)	3181(10)	−430(12)	6882(13)	C(15)	6391(16)	1174(10)	5207(13)
O(2A)	7145(16)	4477(13)	4436(11)	C(16)	5615(16)	918(9)	5426(12)
O(2B)	6079(15)	3656(9)	4004(12)	C(17)	5807(17)	710(11)	6201(16)
O(2C)	6744(17)	4071(11)	3189(12)	C(18)	5044(20)	477(10)	6386(14)
O(2D)	5714(17)	4683(11)	3504(17)	C(19)	4151(18)	478(10)	5859(13)
O(3A)	852(16)	1803(11)	1458(10)	C(20)	3939(17)	704(10)	5041(14)
O(3B)	76(15)	1371(11)	2180(13)	C(21)	4703(18)	902(10)	4889(14)
O(3C)	1504(13)	1833(15)	2802(11)	C(22)	2966(16)	671(10)	4458(14)
O(3D)	254(20)	2472(10)	2139(18)	C(23)	1293(19)	681(13)	4190(16)
N(1)	7462(12)	2774(9)	6212(9)	C(24)	560(17)	876(13)	4530(16)
N(2)	694(14)	1595(10)	4760(10)	C(25)	7896(15)	2646(11)	7101(12)
N(3)	5932(12)	3635(8)	5677(10)	C(26)	7389(18)	2086(12)	7296(12)
N(4)	1361(13)	2769(8)	4422(11)	C(27)	6241(17)	2622(12)	7723(12)
N(5)	6339(13)	1901(9)	5048(9)	C(28)	5236(15)	2754(12)	7599(11)
N(6)	2214(12)	880(9)	4730(10)	C(29)	4944(19)	3394(13)	7674(11)
N(7)	6386(12)	2239(9)	7069(8)	C(30)	3985(20)	3519(15)	7539(13)
N(8)	2116(12)	1951(9)	6269(9)	C(31)	3388(18)	2995(13)	7342(13)
N(9)	4716(13)	2453(8)	5251(9)	C(32)	3632(18)	2361(13)	7266(11)
N(10)	3236(13)	2171(8)	4923(10)	C(33)	4592(19)	2258(14)	7429(11)
C(1)	7603(17)	3468(12)	6062(13)	C(34)	2925(17)	1836(12)	7025(14)
C(2)	6862(16)	3907(13)	6170(13)	C(35)	1328(18)	1498(13)	6248(14)
C(3)	5180(15)	4016(11)	5849(11)	C(36)	490(16)	1674(15)	5513(15)
C(4)	4227(16)	3983(10)	5187(13)	C(37)	4047(17)	2230(9)	5466(12)
C(5)	4063(21)	4222(10)	4426(16)	C(38)	4256(17)	2537(10)	4439(13)
C(6)	3222(23)	4220(11)	3846(16)	C(39)	3345(17)	2360(10)	4231(11)

further effervescence was observed. After 3 h reflux, the mixture was stirred for 2 d at room temperature. After filtering and removal of solvent, the residue was taken up in strong NaOH solution, chloroform-extracted, washed and dried. A waxy solid was obtained in 70% yield, which could be recrystallised from MeOH.

$[Cu_2L^2][ClO_4]_2$ **6**. The cryptand L^2 (0.5 mmol) was dissolved in deoxygenated EtOH (50 cm^3) and $[Cu(MeCN)_4]ClO_4$ (1 mmol) in deoxygenated MeCN (30 cm^3) added. The mixture was heated to 50 °C for 2 h under argon which was then bubbled through the solution to reduce the volume until a cream solid appeared and was filtered off under argon. The product was air-sensitive and turned green rapidly in solution, preventing the acquisition of ^1H NMR spectra. Even as a solid, a green colour was observed within a few days of synthesis. FAB clusters at *m/z* 937 (21, $Cu_2L^2(ClO_4)_2 \cdot H_2O$), 840 [45%, $Cu_2L^2(ClO_4) \cdot H_2O$] and 739 (base peak, $Cu_2L^2 \cdot H_2O$) confirm the formation of the dicopper(I) complex. Yield 52%.

$[Cu_2L^2(OH)][ClO_4]_3 \cdot 3H_2O$ **7**. The cryptand L^2 (0.5 mmol) was dissolved in EtOH–MeCN (1:1, 50 cm^3) and added to $Cu(ClO_4)_2 \cdot 6H_2O$ (1 mmol) in MeCN (20 cm^3). Pyrazole (0.5 mmol) was added as base, and within 2 d slow evaporation in air produced pale blue crystals of **7**. FAB clusters at *m/z* 823 (base peak, $[Cu_2L^2]ClO_4$), 922 [23, $Cu_2L^2(ClO_4)_2$] and 941 {27%, $[Cu_2L^2(OH)][ClO_4]_2$} confirmed the formation of the dicopper(II) μ-hydroxo complex. Yield 57%.

$[Cu_2L^2(N_3)][CF_3SO_3]_3$ **8**. To L^2 (0.5 mmol) in MeCN–EtOH (1:1, 30 cm^3) was added $Cu(CF_3SO_3)_2$ (1.1 mmol) and NaN_3 (0.5 mmol) in H_2O (0.5 cm^3). On mixing, a green solution was produced from which green crystals were isolated after 2 d in 47% yield. FAB clusters at *m/z* 1066 {20, $[Cu_2L^2(N_3)][CF_3SO_3]_2$}, 1023 (25, $[Cu_2L^2][CF_3SO_3]_2$), 916 {12, $[Cu_2L^2(N_3)]CF_3SO_3$} and 873 (35%, $[Cu_2L^2]CF_3SO_3$) confirmed the formation of the dicopper μ-azido complex.

$[Cu_2L^2(im)][ClO_4]_3$ **9**. To L^2 (0.5 mmol) was added imidazole (0.5 mmol) in EtOH–MeCN (1:1, 30 cm^3) and $Cu(ClO_4)_2 \cdot 6H_2O$ (1 mmol) in EtOH (20 cm^3), whereupon a dark blue colour developed. On evaporation, dark blue crystals of **9** were obtained in 54% yield. FAB clusters at *m/z* 992 {base peak, $[Cu_2L^2(im)][ClO_4]_2$}, 924 (41, $[Cu_2L^2][ClO_4]_2$), 823 (65, $[Cu_2L^2]ClO_4$) and 893 [47%, $Cu_2(im)(ClO_4)$] confirmed the formation of the μ-imidazolate dicopper complex.

Physical measurements were made as described in earlier papers.[9]

X-Ray Crystallography.—Complex $5 \cdot H_2O \cdot 0.5EtOH$. $C_{90}H_{96}B_2Cu_2F_3N_8O_6S$, blue-green hexagonal plate, crystal dimensions 0.7 × 0.4 × 0.06 mm, monoclinic, space group $P2_1/a$, a = 17.861(11), b = 17.505(8), c = 26.348(11) Å, β = 91.48(4)°, U = 8235(7) $Å^3$, Z = 4, $F(000)$ = 3404.

Data were collected at 193 K on a Nicolet R3m four-circle diffractometer using graphite-monochromated Mo-Kα radiation (λ = 0.710 73 Å). Using 1.8° ω-scans at 4.2° min^{-1}, 10 215 reflections were collected ($4 < 2\theta < 50°$) and 9850 unique reflections (R_{int} = 0.0923) were used in the refinement. The data were of poor quality, with only 4087 having $I > 2\sigma(I)$. An empirical absorption correction was applied (T_{max} = 0.967, T_{min} = 0.602) and the structure was solved by direct methods[18] which revealed most of the structure of the cation and the BPh_4^- anions. The triflate anion is severely disordered and was inserted with constrained geometry and there is some residual electron density in this region; the ethanol solvate molecule is also disordered about a centre of symmetry. Hydrogen atoms were inserted at calculated positions on the cation and BPh_4^- anions. The non-hydrogen atoms of the cation were refined with anisotropic atomic displacement parameters, except for the carbons of the acetal groups. All the data were used for

refinement on F^2 which converged with conventional $R1 = \Sigma||F_o| - |F_c||/\Sigma|F_o| = 0.119$, $wR2 = \{\Sigma[w(F_o^2 - F_c^2)^2]/\Sigma[w(F_o^2)^2]\}^{\frac{1}{2}}$ 0.275 $[I > 2\sigma(I)]$, $w = [\sigma^2(F_o^2) + (aP)^2]^{-1}$ where $P = \frac{1}{3}[\max(0, F_o^2) + \frac{2}{3}F_c^2]$, goodness of fit = 0.978 for 155 parameters. All programs used in the structure refinement are contained in the SHELXL 93 package.[19] Final atomic coordinates are given in Table 6.

Complex **9**. $C_{39}H_{57}Cl_3Cu_2N_{10}O_{12}$, $M = 1091.4$, monoclinic, space group $P2_1/c$, $a = 15.280(8)$, $b = 20.099(12)$, $c = 18.016(11)$ Å, $\beta = 112.22(4)°$, $U = 5121(5)$ Å^3, $Z = 4$, $D_c = 1.42$ mg m^{-3}, μ(Mo-Kα) = 10.5 cm^{-1}, $F(000) = 2264$, ω-scan, scan width 1.0°, scan range $3 < 2\theta < 40°$.

The crystals were structurally unstable unless sealed in capillaries or with varnish. A scaled hexagonal prism (0.8 mm thick, 0.7 mm edge) gave 4799 unique data on a Siemens P3/V2000 diffractometer; Patterson and Fourier-difference methods (SHELXS 86),[18] full-matrix least-squares refinement (SHELXL 93);[19] anisotropic vibration parameters for all non-hydrogen atoms (except the oxygens of the ClO_4 groups), hydrogens included at positions calculated from the geometry of the molecule; ClO_4 groups in which the oxygens are probably disordered refined as rigid tetrahedra and yielded high isotropic thermal parameters for the oxygen atoms; sample yielded low-quality data (sufficient however to reveal the integrity of the structure) which in the final cycles, using 3052 data with $F_o > 4\sigma(F_o)$, gave $R1 = 0.15$, goodness of fit = 1.01. Final atomic coordinates are given in Table 7.

Additional material available from the Cambridge Crystallographic Data Centre comprises H-atom coordinates, thermal parameters and remaining bond lengths and angles.

Acknowledgements

We thank the Open University Research Committee and the SERC for support (to Q. L. and D. J. M.) and for access to the 400 MHz NMR (Warwick) and FAB mass spectral services (Swansea).

References

1 A. Messerschmidt, A. Rossi, R. Ladenstein, R. Huber, M. Bolognesi, G. Gatti, A. Marchesini, R. Petruzelli and A. Finazzi-Agro, *J. Mol. Biol.*, 1989, **206**, 516; A. Messerschmidt, R. Ladenstein, R. Huber, M. Bolognesi, L. Avigliano, R. Petruzelli and A. Finazzi-Agro, *J. Mol. Biol.*, 1992, **224**, 179; A. Messerschmidt, A. Luecke and R. Huber, *J. Mol. Biol.*, 1993, **229**, 997; A. Romero, C. W. G. Hoitink, H. Nar, R. Huber, A. Messerschmidt and G. W. Canters, *J. Mol. Biol.*, 1993, **229**, 1007; A. Messerschmidt, W. Steigemann, R. Huber, G. Lang and P. M. H. Kroneck, *Eur. J. Biochem.*, 1992, **209**, 597; A. Messerschmidt and R. Huber, *Eur. J. Biochem.*, 1990, **187**, 341.

2 E. I. Solomon, M. J. Baldwin and M. D. Lowery, *Chem. Rev.*, 1992, **92**, 521; E. I. Solomon and M. D. Lowery, *Chemistry of the Copper and Zinc Triads*, eds. A. J. Welch and P. Chapman, RSC, Cambridge, 1993, p. 11; E. I. Solomon, B. L. Henning and D. E. Root, in *Bioinorganic Chemistry of Copper*, eds. K. D. Karlin and Z. Tykelar, Chapman and Hall, New York, 1993.

3 D. McDowell and J. Nelson, *Tetrahedron Lett.*, 1988, 385.

4 D. McDowell, J. Nelson and V. McKee, *Polyhedron*, 1989, **8**, 1143.

5 D. Marrs, V. McKee, J. Nelson and W. Robinson, *Tetrahedron Lett.*, 1989, 7453.

6 (*a*) D. Marrs, M. G. B. Drew, V. McKee and J. Nelson, presented at the First International Conference on the Chemistry of the Copper and Zinc Triads, University of Edinburgh, July 1992; (*b*) D. Marrs, M. G. B. Drew, V. McKee, O. W. Howarth, Q. Lu and J. Nelson, unpublished work.

7 R. Menif, J. Reibenspeis and A. E. Martell, *Inorg. Chem.*, 1991, **30**, 3446.

8 D. Marrs, Ph.D.Thesis, Open University, 1990.

9 D. Marrs, C. J. Harding, N. Martin, Q. Lu, J.-M. Latour, V. McKee and J. Nelson, *J. Chem. Soc., Dalton Trans.*, 1994, 1471.

10 D. Marrs, Q. Lu, V. McKee and J. Nelson, *Inorg. Chim. Acta*, 1993, **211**, 195.

11 Q. Lu, M. McCann and J. Nelson, *J. Inorg. Biochem.*, 1993, 633.

12 Q. Lu, C. Harding, V. McKee and J. Nelson, *J. Chem. Soc., Chem. Commun.*, 1993, 1768.

13 D. Marrs, J. Hunter, C. Harding, M. G. B. Drew and J. Nelson, *J. Chem. Soc., Dalton Trans.*, 1992, 3235.

14 S. J. Archibald, A. L. Blake, M. Schroder and R. E. P. Winpenny, *J. Chem. Soc., Chem. Commun.*, 1994, 1669.

15 C. A. Hunter and J. K. M. Sanders, *J. Am. Chem. Soc.*, 1990, **112**, 5525; P. Hobza, H. L. Selzle and E. W. Schlag, *J. Am. Chem. Soc.*, 1994, **116**, 3500.

16 C.-L. O'Young, J. C. Dewan, H. R. Lilienthal and S. J. Lippard, *J. Am. Chem. Soc.*, 1978, **100**, 7291; A. Bencini, D. Gatteschi, J. Reedijk and C. Zanchini, *Inorg. Chem.*, 1985, **24**, 207; P. Chauduri, I. Karpenstein, M. Winter, M. Lenyan, C. Butzleff, E. Bill, A. X. Trautwein, H. Florke and H. J. Haupt, *Inorg. Chem.*, 1993, **23**, 322.

17 J. L. Pierre, P. Chautemps, S. M. Rejail, C. G. Beguin, A. El-Marzouki, G. Serratrice, P. Rey and J. Laugier, *J. Chem. Soc., Chem. Commun.*, 1994, 1117.

18 G. M. Sheldrick, SHELXS 86, *Acta Crystallogr., Sect. A*, 1990, **46**, 467.

19 G. M. Sheldrick, SHELXL 93, University of Göttingen, 1993.

Received 31*st October* 1994; *Paper* 4/06609J